



# Physicochemical and Functional Characteristics of Saffron (*Crocus sativus* L.) Corm Starch: Gelling and Film-Forming Properties

Mozhgan Esmaeelian<sup>1</sup> · Moslem Jahani<sup>1</sup> · Javad Feizy<sup>2</sup> · Soodabeh Einafshar<sup>3</sup>

Received: 11 April 2022 / Accepted: 25 June 2022 / Published online: 30 June 2022  
© The Author(s), under exclusive licence to Springer Science+Business Media, LLC, part of Springer Nature 2022

## Abstract

In the present study, isolated starch from the saffron corm (SS) was investigated for physicochemical and functional properties and compared with the potato (PS) and waxy rice starches (RS). The SS granules were irregular and heterogeneous in appearance with bimodal particle size distribution. A mean granule size of 2.66, 8.87, and 32.27  $\mu\text{m}$  (Dv50) was recorded for RS, SS, and PS granules, respectively. The lowest degree of crystallinity and the least gelatinization enthalpy of SS are linked to its high amylose/amylopectin ratio. The least swelling power was obtained for SS gel and followed by RS and PS gels. Also, SS and RS samples showed the most syneresis and paste turbidity. Higher viscoelastic solid properties, gel strength, and final viscosity were also observed in the SS gel. The elastic modulus of saffron corm starch gel was less frequency dependent than potato and waxy rice starches. The most heterogeneous film was prepared from SS with the least transparency and maximum thickness. Also, the lowest film transparency was obtained for the rice starch sample. The SS films had the highest maximum tensile strength and stiffness but the lowest film stretchability. So, the saffron corm starch can be used when higher gelling properties or less transparency and more rigid films or coatings are required.

**Keywords** Edible film · Amylose · Rheological properties · Textural properties

## Abbreviations

CP	Swelling power
DSC	Differential scanning calorimeter
PS	Potato starch
RH	Relative humidity
RS	Rice starch
SD	Standard deviation
SE	Standard error
SS	Saffron corm starch
TPA	Texture profile analysis
TS	Tensile strength

## Introduction

Starch, the major storage polysaccharide in plants, is a heterogeneous composite of two polyglucans, amylose and amylopectin, both of which are characterized by  $\alpha$ -linked D-glucosyl units [1]. The native starch granules exhibited an annular structure of alternant crystalline and semicrystalline layers. The crystallites are formed by short, external chain segments of amylopectin. In the A-type crystal, the double-helices are closely packed into a monoclinic unit cell containing 8 water molecules. In the B-type crystal, the double-helices are packed in a hexagonal unit cell with 36 water molecules. Also, some plants possess granules with a mixed pattern assigned C-type [2]. In addition to non-food applications, starch is an important food ingredient increasingly used to enhance the product texture, quality, and stability during storage. It serves as a significant source of human energy and is used in many kinds of food products like soups, sauces, canned foods, beverages, jams and jellies, syrups, and dairy products [3].

Some unconventional resources contain significant amounts of starch and can introduce starches with unique characteristics and desired functionality for specific applications [4]. The uses of starch are dependent on its

✉ Moslem Jahani  
m.jahani@rifst.ac.ir; moslemjahani@yahoo.com

<sup>1</sup> Department of Food Chemistry, Research Institute of Food Science and Technology (RIFST), P.O. Box: 91895-157-356, Mashhad, Iran

<sup>2</sup> Department of Food Safety and Quality Control, Research Institute of Food Science and Technology (RIFST), Mashhad, Iran

<sup>3</sup> Agricultural Engineering Research Department, Khorasan Razavi Agricultural and Natural Resources Research and Education Center, AREEO, Mashhad, Iran

physicochemical properties like granule morphology, degree of crystallinity, amylose content, retrogradation resistance, viscosity properties, and nutritional characteristics [5].

Torruco-Uco and Betancur-Ancona (2007) studied the physicochemical and functional properties of makal starch, a potentially useful tuber found in the southeast of Mexico. The results showed an amylose content of 22.4% with high starch purity (96.7%), low protein (0.1%), fat (0.2%), fibre (0.4%) and ash (0.1%) contents. The makal starch has high gelification temperature and firmness, making it appropriate for use in high-temperature food systems [4].

The physicochemical properties of starches isolated from four traditional Taewa (Maori potato) cultivars (Karuparera, Tutaekuri, Huakaroro, and Moemoe) of New Zealand were also studied and compared with modern potato cultivars (Nadine). The results showed that Nadine and Moemoe cultivars have large and irregular or cuboid granules in fairly high numbers compared to other cultivars. The transition temperatures and the gelatinization enthalpies suggested differences in the stability of the crystalline structures among these starches. Also, the lowest tendency toward retrogradation was observed for Nadine and Huakaroro starch gels [6]. The physicochemical properties of pumpkin starch were evaluated compared to potato and corn starches. The results showed a similar syneresis of pumpkin starches to potato starch but much lower than that for corn starch. Pumpkin starches have lower pasting temperatures (17–21.7°C). The final viscosities were over 1000 cP higher than corn paste but close to the values obtained for potato starch. The lowest retrogradation level (32–48%) was recorded for pumpkin starches and followed by corn (59%) and potato (77%) starch samples. The pumpkin starches gels were characterized by a much greater hardness, cohesiveness and chewiness, than potato or corn starches gels [7].

As the most expensive spice in the world, saffron is the dried stigma of *Crocus sativus* L. *C. sativus* is propagated vegetatively through corms, and a positive relationship was reported between the corm size and saffron yield [8]. Because of the restricted flowering potential, small corms (less than 8 g) are not appropriate for replanting, and large amounts of small corms are generated annually [9]. Therefore, new strategies are desirable for better management of small corms as a by-product of saffron production.

Like most bulbous plants, saffron corms are rich in carbohydrates. During sprouting progress, starch accumulation decreases progressively while no significant changes are observed during the dormancy period [10]. Small saffron corms can be considered as a potential source of starch which can add extra income to the farmers.

In this sense, this study aims to characterize the starch extracted from the saffron corm (SS). Also, SS was compared with the potato (PS) and rice (RS) starches used as control samples. PS was selected as a starch widely used

in the food industries, obtained from tubers of roots. Also, the correlations between physicochemical, gelling, and film formation characteristics and amylose content have been studied in SS, PS, and waxy rice starch. Although potato and rice starches are readily available and commonly used in food processing, there is a lack of information on the properties of saffron corm starch. So, this work aims to measure the physicochemical and functional properties of the saffron corm starch like composition, crystallinity, gelatinization behaviour, swelling, pasting, and film formation.

## Materials and Methods

### Samples

The saffron corms were collected during July 2018 from a local farm in the Torbat-e Heydarieh farming zone in Khorasan Razavi Province, Iran. At first, the corms were cleaned and depleted from their sheathing tunics and washed with tap water.

### Chemicals

Iodine standard solution and glycerol were acquired from Sigma-Aldrich (Sternheim, Germany). Sodium metabisulfite, sodium hydroxide (NaOH), and potato starch (PS) were obtained from Merck (Darmstadt, Germany). Commercial native rice starch (RS) was also acquired from CDH Fine Chemicals (India). Hydrochloric acid (HCl), ethanol, acetone, toluene, and other chemicals were obtained from Merck or Sigma. All chemicals and reagents were of analytical grade and used as received.

### Extraction of Saffron Corm Starch

The saffron corm starch was extracted using a previously described method with slight modification [6]. The cleaned saffron corms were peeled into small slices and mixed with a sodium metabisulphite solution (0.35 g/L) using a mixer grinder. The resulting slurry was filtered using a 100-mesh (150- $\mu$ m) sieve followed by washing the residue with distilled water (3 times). Then, the slurry was settled for 4 h and, the supernatant was decanted. The white starch sediment was re-dispersed in distilled water and shaken for 30 min. The starch suspension was allowed to settle, and the washing step was repeated five times. Finally, the purified starch was dried at 35°C for 24 h and was kept in a sealed container at room temperature (23.0–25.0°C) until further use. The extraction yield was calculated according to Eq. (1).

$$\text{Starch extraction yield(\%)} = \frac{\text{SS}}{\text{SC}} \times 100 \quad (1)$$

Where ‘SS’ and ‘SC’ are the weight (g) of the extracted starch and initial saffron corm, respectively [11].

## Characterization of Starch Granules

### Proximate Composition and Amylose Content

Starch samples were analyzed for their crude protein ( $N \times 6.25$ ), fat, and ash following the standard analysis methods [12].

The amylose content was determined using the iodine colorimetry method [13]. Briefly, 0.1 g of starch sample was mixed with 1.0 mL ethanol and 9.0 mL sodium hydroxide solution (1.0 mol/L) and heated in a water bath for 10 min. When cooled to room temperature, the sample was diluted to 100 mL. Then, 1.0 mL of acetic acid (1.0 mol/L) and 2.0 mL iodine solution were added to 5.0 mL of the starch sample and thoroughly mixed. The absorbance (Abs.) was determined at 620 nm and, the amylose content was calculated according to Eq. (2).

$$\text{Amylose content(\%)} = 3.06 \times \text{Abs.} \times 20 \quad (2)$$

### Granule Color and Particle Size

The finely grounded starch samples were taken in a Petri dish, and the colour parameters of ‘L\*’, ‘a\*’, and ‘b\*’ were determined using a Minolta colorimeter CR-200 (Minolta Co. Ltd., Osaka, Japan). The final results were expressed as the total colour change ( $\Delta E$ ).

The particle size distribution was measured using an Analysette 22 particle size analyzer (Fritsch, Germany). Water was used as a dispersing medium and, suspensions were subjected to sonication before measurements for better dispersion. The refractive index values of 1.33 and 1.41 were used for water and starch, respectively. Particle size distribution was expressed as 10, 50 and 90% volume-based size (Dv10, Dv50, and Dv90, respectively) [14].

### Optical and Scanning Electron Microscopy

One uniform drop of the starch suspension (3%w/v), prepared in a water-glycerol mixture (1:1), was placed on a coverslip and covered with another coverslip. The prepared samples were examined with an OLYMPUS BX60 (Olympus, Japan) optical microscope at  $\times 40$  magnification. The surface morphology of starch granules was determined using an LEO 1450VP scanning electron microscope (Carl Zeiss, Germany) at an accelerating voltage of 20 kV. The

size distribution of starch granules is estimated from the micrographs at  $\times 750$  magnification.

### X-ray Diffraction Characterization

The X-ray diffraction (XRD) patterns of starch granules were recorded on a GNR Explorer X-ray diffractometer (GNR analytical instruments, Italy) operating at 35 kV and 15 mA, with a  $\text{CuK}\alpha$  radiation wavelength of 1.54 Å and from 4° to 35° on a 2θ scale with a step size of 0.02°. The crystallinity degree was calculated as the ratio of the crystalline area and the total area covered by the XRD curve [13].

### Swelling Power and Light Transmittance

A starch slurry, prepared in distilled water (2.5%w/v), was heated at different temperatures (60–90°C) in a thermostatically regulated water bath for 30 min. It was cooled to room temperature and centrifuged at 2000 rpm for 15 min. The swelling power (CP), expressed as g/g, was calculated as the weight ratio of the swollen starch to the initial dry weight [15]. The temperature dependency of CP was predicted by the power-law model expressed in Eq. (3).

$$Y = Y_0 + a(T - T_{\text{ref}})^b \quad (3)$$

Where ‘a’ and ‘b’ are model constants and ‘y’ and ‘y<sub>0</sub>’ are the weight of starch sample at test (T) and reference (T<sub>ref</sub> = 60°C) temperatures, respectively.

An aqueous suspension (1%w/v), heated at 100°C for 30 min with intermittent mixing, was used to determine the turbidity of starch paste. The paste was transferred into a disposable cuvette, cooled down to room temperature and stored at 4°C for five days. The transmittance (%) was measured at 650 nm using a DR 500 UV–Vis spectrophotometer (Hach, USA) every 24 h and with water as blank. The time dependency of turbidity of starch pastes was predicted by the power-law model as expressed in Eq. (4).

$$Y = a + b(x)^c \quad (4)$$

In Eq. (4), ‘a’, ‘b’, and ‘c’ are model constants and ‘x’ is the storage time (h).

## Physicochemical Properties of Starch Gel

### Thermal Properties

The starch sample ( $3.5 \pm 0.5$  mg) was weighed into the 40 μL standard aluminium pan and, distilled water was added to give a 25%w/v starch suspension. Samples were hermetically sealed and allowed to stand for 24 h before differential scanning calorimetric analysis (DSC, Diamond, PerkinElmer, USA). The sample and an empty (reference) pan

were heated from 25 to 110°C at a heating rate of 10°C/min. The DSC thermograms were used to determine onset temperature ( $T_0$ ), peak temperature ( $T_p$ ), and gelatinization enthalpy ( $\Delta H_{\text{gel}}$ ) [13].

### Syneresis

The starch suspension (6%w/v) was heated at 90°C for 30 min with continuous stirring, followed by rapid cooling to room temperature (23.0–25.0°C) using an ice water bath. The samples were stored at 4.0°C for five days for the syneresis measurement. Syneresis is calculated as the weight percentage of released water after centrifugation at 2000 rpm for 10 min [7]. The time dependency of syneresis of starch pastes was predicted using the Power-law model as expressed in Eq. (5).

$$Y = a(x)^b \quad (5)$$

Where ‘a’ and ‘b’ are model constants and ‘x’ is the storage time (h).

### Pasting Properties

Pasting properties and viscosity profiles were measured by a Rapid Visco Analyzer (RVA-4, Newport Scientific, Warriewood, Australia). The starch suspension (8%w/v) was heated from 50 to 95°C, at a heating rate of 12.5°C/min, held for 5 min and finally cooled down to 50°C, under a similar cooling rate. The samples were stirred at 960 rpm for the first 1 min and 160 rpm for the rest of the testing time [14].

### Rheological Properties

The elastic ( $G'$ ) and viscous ( $G''$ ) modules of starch pastes and starch gels (15%w/v) were measured using Physica MCR 301 Rheometer (Anton Paar, Austria) with plate and plate parallel geometry (PP 25).

In the temperature sweep tests, the shear stress and frequency were set at 1 P and 1 Hz, respectively. The starch suspension was thoroughly mixed at  $60 \pm 2^\circ\text{C}$  and poured on the lower plate of the rheometer, previously maintained at 60°C. The temperature was raised from 60 to 90°C, at a heating rate of 2°C/min, held for 10 min and cooled down to 60°C, at the same cooling rate. The storage ( $G'$ ) and loss modulus ( $G''$ ) of the gels were recorded as a function of temperature within the linear viscoelastic regime.

Dynamic frequency sweep tests were conducted in situ and after the temperature sweep test. Frequency sweep was run from 0.001 to 10 Hz at a shear stress of 10 Pa at 60°C. The degree of frequency dependence expressed by the constant ‘n’ was calculated by Eq. (6).

$$G' = Kf^n \quad (6)$$

In Eq. (6), ‘K’ and ‘n’ are the corresponding fitting parameters,  $G'$  is the storage modulus (Pa), and ‘f’ is the oscillation frequency (Hz). The constant ‘n’ is the slope of log  $G'$  versus log f plot [16].

### Texture Profile Analysis

Texture profile analysis (TPA) of starch gels was carried out using a CT3 texture analyser (Engineering Laboratories, Middleboro, MA, USA). The starch paste (Section 2.5.5) was prepared in the plastic tube and heated in a water bath (90°C) for 10 min and under continuous mixing. It was poured into a silicone mold and immediately cooled under tap water. The gel was stored at 4°C overnight and equilibrated to room temperature (23.0–25.0°C) for at least 30 min before analysis. The resulting gel was cut into cylinders (8 mm in diameter and height) then was compressed to 30% of its original height at a constant speed of 0.3 mm/s, using a TA10 cylindrical probe, in two compression cycles. The TPA analysis was carried out on load–time curves to calculate hardness, cohesiveness, adhesiveness, springiness, resilience, and gumminess.

### Characterization of Starch Films

#### Film Formation

Starch films were prepared by the casting method. A starch suspension (4%w/v) was prepared in distilled water, followed by the addition of glycerol (2%w/v) under mixing at 300 rpm. The mixture was heated in a water bath (80°C) for 25 min and under continuous stirring. When cooled to 60°C, gelatinized starch (70 mL) was poured into polystyrene Petri dishes and dried in a UF110 Universal oven (Memmert GmbH, Schwabach, Germany) at 35°C for 48 h. The films were separated from Petri dishes after conditioning for five hours at room temperature and kept in polyethylene bags for further treatments.

#### Light Transparency

The starch films were cut into  $4 \times 1$  cm rectangular, and the absorbances were recorded at 600 nm. The film’s transparency was calculated according to Eq. (7).

$$\text{Transparency} = \frac{A_{600}}{x} \quad (7)$$

In Eq. (7),  $A_{600}$  is the absorbance at 600 nm, and  $x$  is film thickness (mm). The film thickness was measured using a digital micrometre screw gauge with an accuracy of 0.001 mm (Mitutoyo Digital Micrometer, Series -193).

## Film Stability in Water

Starch films (2×3 cm) were stored in a desiccator (0% RH) for seven days. The films were transferred to beakers containing 25 mL of deionized water and agitated for 1 h at room temperature. Then, the starch films were dried at 60°C, and total soluble matter (% solubility) was calculated according to Eq. (8).

$$\% \text{Solubility} = \frac{m_1 - m_2}{m_1} \times 100 \quad (8)$$

Where,  $m_1$  and  $m_2$  are the initial and final dry weight of starch films, respectively [17].

## Mechanical Properties

The starch films were stored at a relative humidity (RH) of  $50 \pm 2\%$  and 25°C and for 24 h to reach a constant weight. Mechanical properties were evaluated with 10×90 mm strips, using a texture analyzer (SMS TA-XT2, UK) at an initial distance of 80 mm between the grips and a test speed of 12.5 mm/min. The tensile strength (TS, MPa) and elongation at break (E, %) were calculated according to Eqs. (9) and (10), respectively [18].

$$\text{TS} = \frac{L_p}{a} \times 10^{-6} \quad (9)$$

$$E = \frac{\Delta L}{L} \times 100 \quad (10)$$

Where  $L_p$  is the peak load (N),  $a$  is the cross-sectional area of the sample ( $\text{m}^2$ ),  $\Delta L$  is the elongation at breaking point (mm), and  $L$  is the original length (mm).

## Statistical Analysis

Statistical analysis was conducted using SPSS Statistics 19.0 software (SPSS Co., Chicago, U.S.). One-way analysis of variance (ANOVA) and Duncan's post hoc was used to compare data and, the P-values less than 0.05 were considered statistically significant.

## Results and Discussion

### Physicochemical Properties of Starch Granules

#### Chemical Composition and Color

Isolation of starch from saffron corm with sodium metabisulphite solution achieved an extraction yield of  $43.38 \pm 1.21\%$ . As presented in Table 1, the ash and crude protein content ranged from 0.18 to 0.27 g/100 g and 0.79 to 2.61 g/100 g, respectively. Also, SS and PS showed lower protein contents than RS. The lower ash and protein contents indicate more starch purity.

The results showed significant differences ( $p < 0.05$ ) in amylose content and the highest amylose was recorded for SS and followed by PS and RS (Table 1). The functional properties of starches are affected by amylose content. High amylose content suggests susceptibility to retrogradation and higher paste elasticity [19].

**Table 1** Physicochemical properties of the saffron corm, potato, and rice starch samples

Parameters		SS	PS	RS
Ash (g/100 g)		$0.188 \pm 0.005^c$	$0.215 \pm 0.001^b$	$0.271 \pm 0.013^a$
Protein (g/100 g)		$0.833 \pm 0.050^b$	$0.793 \pm 0.005^b$	$2.616 \pm 0.060^a$
Fat (g/100 g)		$0.898 \pm 0.057^a$	$1.002 \pm 0.104^a$	$1.032 \pm 0.089^a$
Amylose (%)		$31.631 \pm 2.139^a$	$14.453 \pm 0.244^b$	$0.000 \pm 0.000^c$
Relative crystallinity (%)		$28.28 \pm 0.59^c$	$31.46 \pm 0.57^b$	$43.80 \pm 0.48^a$
Color parameters	L*	$82.96 \pm 1.75^a$	$82.43 \pm 5.31^a$	$87.87 \pm 1.54^a$
	a*	$0.27 \pm 0.02^a$	$-0.05 \pm 0.03^b$	$-0.37 \pm 0.05^c$
	b*	$4.10 \pm 0.22^a$	$2.86 \pm 0.22^b$	$2.29 \pm 0.11^c$
	$\Delta E$	$83.06 \pm 1.76^a$	$82.47 \pm 5.31^a$	$87.90 \pm 1.54^a$
Starch granule size ( $\mu\text{m}$ )	Dv10	$2.01 \pm 0.005^b$	$8.53 \pm 0.055^a$	$0.74 \pm 0.005^c$
	Dv50	$8.87 \pm 0.020^b$	$32.27 \pm 0.015^a$	$2.66 \pm 0.020^c$
	Dv90	$38.15 \pm 0.110^b$	$50.09 \pm 0.020^a$	$6.11 \pm 0.015^c$
Gelatinization properties	$T_0$ (°C)	$68.92 \pm 0.43^a$	$60.80 \pm 0.10^c$	$63.42 \pm 0.39^b$
	$T_p$ (°C)	$74.11 \pm 0.08^a$	$69.10 \pm 0.11^c$	$70.16 \pm 0.06^b$
	$\Delta H_{\text{gel}}$ (J/g)	$11.69 \pm 0.05^c$	$13.36 \pm 0.15^b$	$15.33 \pm 0.09^a$

Data are expressed as mean  $\pm$  SD ( $n = 3$ )

Means with different superscript letters within the same row are significantly different ( $p < 0.05$ )



As documented in Table 1, there were significant differences among starch samples regarding  $a^*$  and  $b^*$  values while  $L^*$  and  $\Delta E$  values were similar. Higher  $L^*$  and lower  $b^*$  values may result from higher protein content of RS [20]. Pigments and polyphenolic compounds have also a considerable impact on starch characteristics. The presence of pigments can reduce the quality and acceptability of the starch final product, and a higher lightness value is desirable for starch to meet consumer preference [21].

### Granules Morphology and Size Distribution

The morphological characteristics of starch granules depend on the plant source, agronomic and climatic conditions, and metabolic routes occurring in the chloroplast or amyloplast [22]. Based on SEM and light microscopic images, the RS granules are small and polygonal in shape (Fig. 1a), SS granules are irregular and heterogeneous in appearance (Fig. 1b), and PS granules are large oval to small round (Fig. 1c). All starch granules showed a smooth surface without any fissures that confirmed the removal of all other cellular residues.

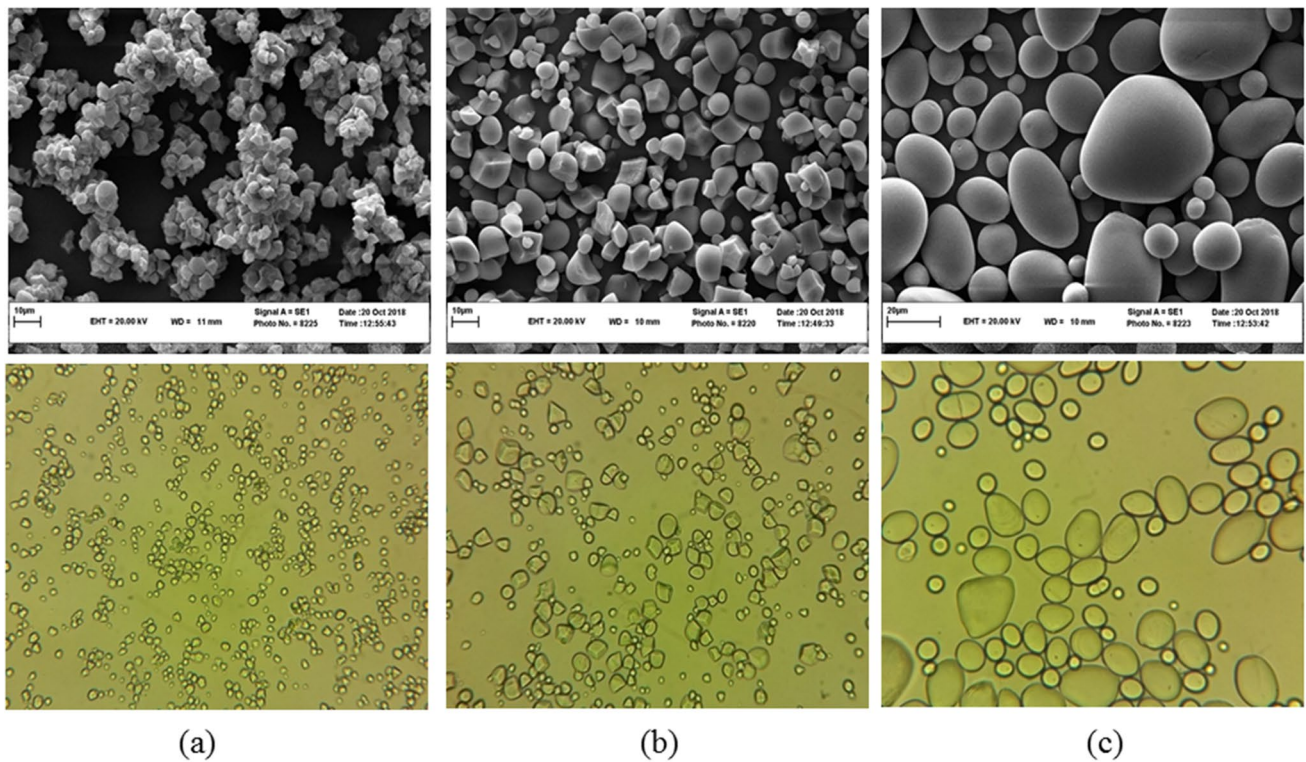


**Fig. 1** SEM and optical microscopy micrographs of RS (a), SS (b), and PS (c) granules and particle size distribution pattern of starch samples (d)

The granule size affects starch functionality because the larger granules tend to more swelling during cooking. As presented in Fig. 1d, the PS showed the highest mean granule size, while the RS has the smallest granules. SS exhibited bimodal particle size distribution with the mean granule size of 8.87  $\mu\text{m}$  (Dv50). PS and RS granules showed monomodal size distribution with the mean granule size of 32.27  $\mu\text{m}$  and 2.66  $\mu\text{m}$ , respectively (Table 1). These size distribution data for PS and RS are within the range of other published data [23].

### X-ray Analysis

The supramolecular complex of amylose and amylopectin forms partially crystalline granules. Starch granules have hexagonal (B-type starch) and/or orthorhombic (A-type starch) nanocrystals. The C pattern is very similar to the A pattern, except for the appearance of a peak around  $5^\circ 2\theta$ . The type of diffraction pattern primarily depends upon the arrangement of the double-helical amylopectin chains [24].

The d spacing was computed according to Bragg's law of diffraction and reported in angstroms,  $\text{\AA}$ . As presented in Fig. 2, potato starch has its diffraction peaks at around  $15.4^\circ$  (5.75  $\text{\AA}$ ),  $17.3^\circ$  (5.15  $\text{\AA}$ ),  $18.8^\circ$  (4.72  $\text{\AA}$ ), and  $23.4^\circ$  (3.78  $\text{\AA}$ )  $2\theta$ . The pattern of peaks seen in the diffractogram of PS is characteristic of a B-type crystalline structure. RS sample has the strongest peaks at approximately  $15.3^\circ$  (5.75  $\text{\AA}$ ),  $17.2^\circ$  (5.09  $\text{\AA}$ ), and  $23.2^\circ$  (3.83  $\text{\AA}$ )  $2\theta$ . Moreover, the peak at  $18.2^\circ 2\theta$  is unresolved and has been converted into a shoulder, a feature characteristic of an A-type pattern. Also, saffron corm starch has its strongest diffraction peaks at around  $15.3^\circ$  (5.78  $\text{\AA}$ ),  $17.4^\circ$  (5.06  $\text{\AA}$ ),  $18.1^\circ$  (4.89  $\text{\AA}$ ), and  $23.2^\circ$  (3.83  $\text{\AA}$ )  $2\theta$ , and relatively medium/weak peaks at around  $4.8^\circ$  (18.02  $\text{\AA}$ ) and  $19.1^\circ$  (4.64  $\text{\AA}$ )  $2\theta$  and can be assigned to C-type crystalline structure.

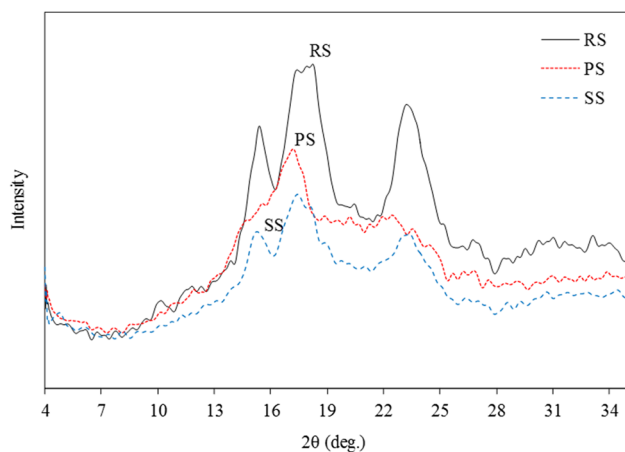


**Fig. 2** X-ray diffraction patterns of studied starch samples

The degree of crystallinity is a valuable parameter that influences the properties of the starch or starch-containing products. The results confirm the different crystallinity of the samples (Table 1). As presented by Kim et al., (2015), the relative crystallinity of the starch nanoparticles increased as the amylose content decreased. Also, in starches having similar contents of amylose but different botanic origins, no significant differences were observed in the degree of crystallinity [25]. The extraction method can also alter the crystallinity. Longer extraction times promoted the swelling of the starch granules and more amylose could be leached out [26].

### Starch Granule Swelling Power

Swelling power is not only a measure of the hydration capacity of the sample but is also indicative of the associative forces in the granules. This process requires the prior loss of at least some of the ordered structures within the native granule and is often regarded as the final stage in the gelatinization process [27]. When starch is heated beyond the gelatinization temperature, granules swell up to many times their original size, collapse and release amylose in the continuous medium. The swelling behavior was investigated over a temperature range of 60–90°C and showed an increase in swelling power by raising the temperature. The SS showed notably lower swelling power at temperatures beyond 60°C, while PS and RS exhibited higher swelling power (Fig. 3a). The dependence of swelling power on temperature for waxy and normal rice starches is also reported [28]. Some starches, like grains, show very little water uptake at room temperature and small swelling power. At higher temperatures, water uptake increases and starch granules collapse. This leads to solubilization of amylose and amylopectin and form a colloidal solution. Hence the increase in moisture absorption with the increase in temperature.

Swelling of starch is primarily a function of amylopectin and the amylose can act as an inhibitor of starch granule swelling and hinder the disruption of amylopectin double helices [26]. So, starches with lower amylose content would have higher swelling power and solubility. The presence of non-polysaccharide material like lipids and proteins at or near the surface of the granule is another potential mechanism for restraining the rate and extent of starch swelling [29]. Partial defatting or partial protein removal results in an enhanced rate and extent of granule swelling. The swelling power as a function of temperature was also predicted using the Power-law model, as shown in Fig. 3a. The swelling behaviour of starch samples was perfectly predicted by this model (Table 2).

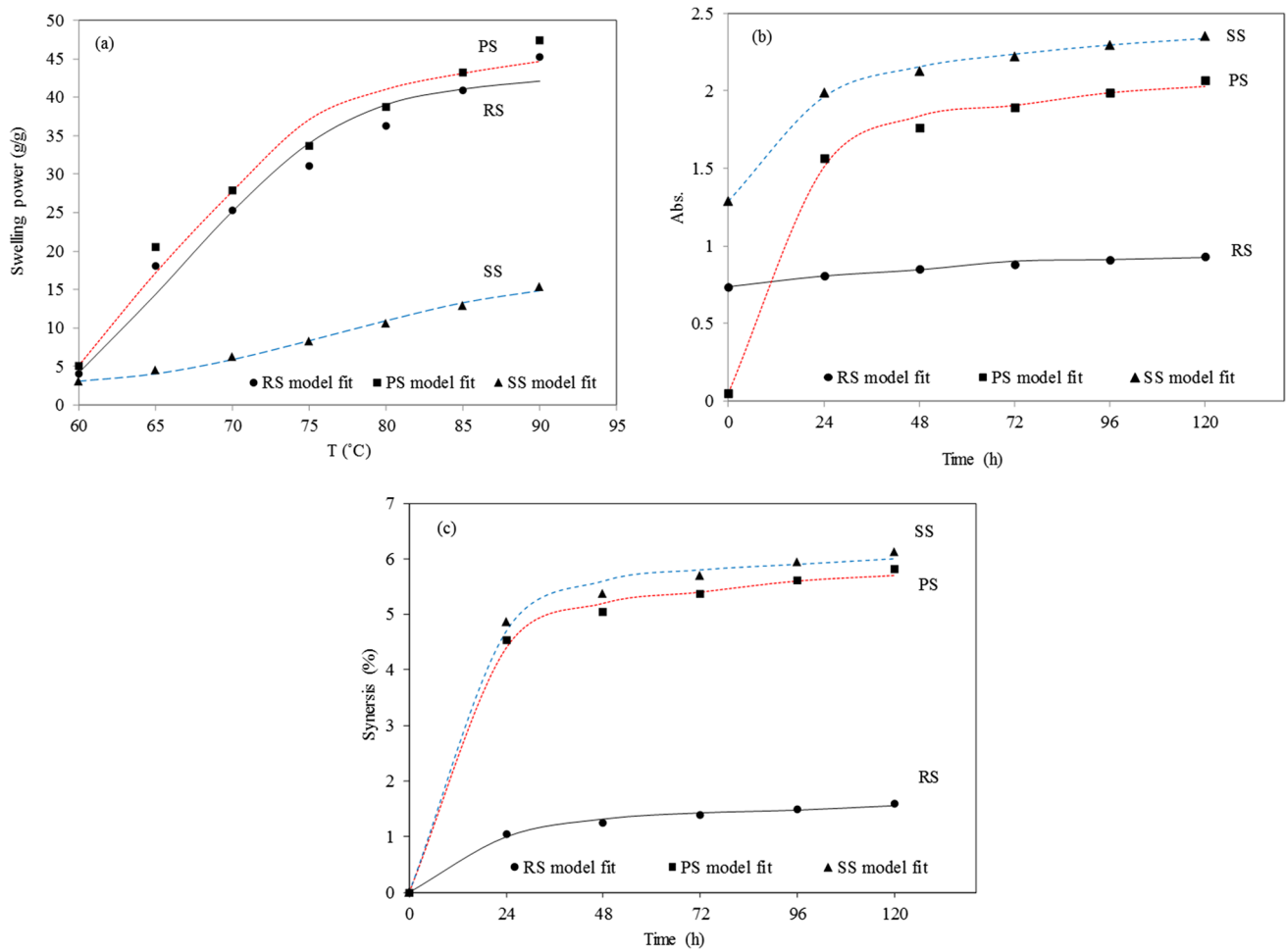


**Fig. 3** Experimental and model fitted data of swelling power (a), paste turbidity (b), and paste syneresis (c) (Markers show the model fitted to the experimental data)

**Table 2** Model fitting parameters of swelling power, paste turbidity, and syneresis

	Model fitting parameters	SS	PS	RS
Swelling power	a	0.186	6.28	5.25
	b	1.23	0.561	0.605
	SE	0.419	2.664	2.799
	R <sup>2</sup>	0.992	0.973	0.969
Paste turbidity	a	1.29	0.052	0.734
	b	0.301	0.855	0.011
	c	0.264	0.179	0.589
	SE	0.026	0.058	0.013
	R <sup>2</sup>	0.997	0.996	0.980
Syneresis	a	3.1	2.78	0.47
	b	0.142	0.154	0.254
	SE	0.163	0.116	0.048
	R <sup>2</sup>	0.996	0.997	0.994

SE: standard error

## Physicochemical Properties of Starch Gel

### Gelatinization Properties

The thermal properties of starch are related to a variety of factors, including amylose content, crystalline structure, and protein and lipid contents. The crystallinity lamellae of starch granules require higher energy for gelatinization than the amorphous lamellae [27]. Starch gelatinization properties are important to understand the chemical composition and potential applications [22]. As presented in Table 1, the SS has the highest onset (68.92°C) and peak (74.11°C) gelatinization temperature, while PS has the lowest.

The lowest (11.69 J/g) and highest (15.33 J/g) gelatinization enthalpies were recorded for SS and RS, respectively (Table 1). Also, the degree of crystallinity and gelatinization enthalpy followed the same order. Accordingly, the lower gelatinization enthalpy for SS might be due to its low crystallinity. The gelatinization enthalpy reflected both



crystalline order and the level of amylopectin double-helical order. A longer chain in amylopectin would result in longer crystallites and take more thermal energy to break. Also, A-type crystallinity usually has a higher gelatinization temperature than B-type crystallinity [30].

### Paste Turbidity

Paste clarity, the capacity to transmit light, may be affected by various factors such as amylose, lipid and protein contents, botanical source, granules particle size, total solids concentration, degree of granule dispersion, and capacity of granules to form aggregates [31].

The results represented an increase in turbidity during the storage at 4 °C, mainly due to continued interaction between leached amylose and amylopectin chains. To a lesser extent, the same behaviour can result from the short-range ordering of amylopectin side chains, development of functional zones which significantly reflect or scatter the light [32]. As presented in Fig. 3b, the RS has better storage stability (absorbance 0.7–0.9). The higher amylose content leads to rising in turbidity because the starch is more difficult to disperse [33]. The high initial clarity of PS paste may be due to its higher swelling power, the repulsion between negatively charged phosphate groups in the amylopectin chain and the absence of granule fragments [32].

The paste turbidity as a function of time was also predicted using the Power-law model (Fig. 3b) that remarkably predicted the turbidity behaviour of starch samples (Table 2).

### Syneresis

Syneresis, an index of starch retrogradation at low temperatures, is an undesired property for both food and non-food applications [23]. As presented in Fig. 3c, the highest (up to 6%) and lowest syneresis (<2%) were recorded for SS and RS pastes, respectively. The paste syneresis as a function of time was predicted using the Power-law model that excellently predicted the behavior of all pastes ( $R^2 > 0.99$ ).

Another study reports syneresis values of 13.6% and 2.0% during the first four days of storage for the corn and potato starch paste, respectively [7]. Also, syneresis in the range of 0.04% to 2.41% for nonwaxy rice starches stored at 4 °C for 48 h was informed [34]. An increase in syneresis may be resulted from increased molecular hydrogen bonding and aggregation of starch chains during storage, leading to water releases.

### Pasting Properties

Figure 4 shows the RVA viscosity profile of starch pastes and the pasting properties are listed in Table 3. Among samples, PS exhibited the highest peak viscosity (8918 cP) at

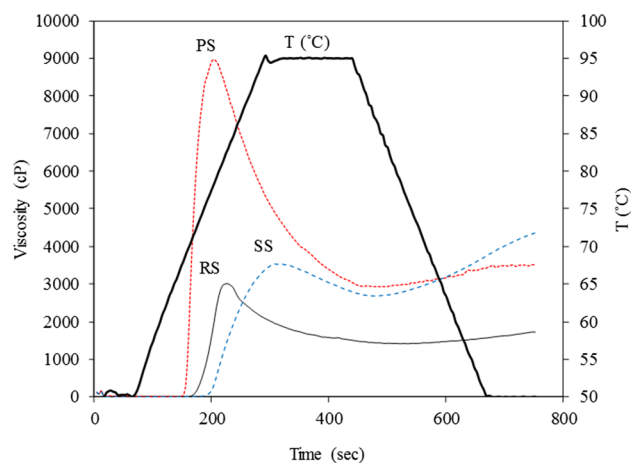


**Fig. 4** RVA viscosity profile of starch pastes at 12.5 °C/min heating and cooling rate (standard protocol)

the shortest time (204 s). The shorter time of peak viscosity shows the PS is the more easy-to-cook starch than SS and RS. Peak viscosity reflects the ability of starch granules to bind water and can be affected by different parameters like starch water concentration, amylose content, lipids, residual proteins, granule size, amylopectin structure and operating conditions of the instrument. For instance, two wheat starches with similar amylose content and similar amylopectin crystallinity showed different peak viscosity and higher phospholipid content was associated with a lower peak viscosity, indicative of lower swelling [29, 30]. The RS and SS samples showed higher thermal stability. High-amylose starches contain more amounts of long chains, which can delay the starch gelatinization by strengthening the stability of crystals. So, high-amylose starches showed higher pasting temperatures [35].

The increase in viscosity of a heated starch paste is attributed to the release of an exudate (predominantly amylose) and folding (deformation) of the swollen starch granules [36]. SS showed the longest peak time (time taken by a sample to reach peak viscosity) which shows its less ability to water adsorption and swelling [36]. Heating starches beyond the point of peak viscosity, with continuous shearing, leads to a decrease in viscosity. Breakdown viscosity can evaluate the starch pasting resistance to heat with lower value having higher ability to withstand heating, and setback viscosity reflects the tendency of starch paste to retrogradation. So, the lowest break-down viscosity of SS is related to its higher heat stability.

In the pasting curve, increasing viscosity from the breakdown to the final equilibrium viscosity value is known as a setback. The SS paste displayed the highest final viscosity which means higher stability of swollen granule structure and greater stability for stirring and cooking. Also, the order of final viscosity matches the amylose content. The amount

**Table 3** Pasting properties of studied starch samples

Parameters	SS	PS	RS
Peak viscosity (cP)	3507.66 ± 31.64 <sup>b</sup>	8918.33 ± 62.74 <sup>a</sup>	3064.33 ± 116.07 <sup>c</sup>
Peak temperature (°C)	94.86 ± 0.35 <sup>a</sup>	78.24 ± 0.05 <sup>c</sup>	82.91 ± 0.04 <sup>b</sup>
Peak time (sec)	314.00 ± 2.64 <sup>a</sup>	201.66 ± 2.08 <sup>c</sup>	227.33 ± 2.08 <sup>b</sup>
Break down viscosity (cP)	829.66 ± 5.50 <sup>c</sup>	6058.00 ± 45.07 <sup>a</sup>	1580.33 ± 5.68 <sup>b</sup>
Set back viscosity (cP)	1637.33 ± 38.00 <sup>a</sup>	574.66 ± 6.65 <sup>b</sup>	300.00 ± 2.64 <sup>c</sup>
Final viscosity (cP)	4362.66 ± 9.07 <sup>a</sup>	3492.00 ± 8.54 <sup>b</sup>	1747.00 ± 60.50 <sup>c</sup>

of leached amylose, starch nature, and applied shear rate affects final-viscosity [37]. Accordingly, the saffron corn starch can be appropriate when strong gelling properties are required in the final product.

**Dynamic Rheological Characteristics of Starch Gels**

The effect of heating on the storage modulus ( $G'$ ) is presented in Fig. 5a. PS had the shortest gelation time, the time at which the  $G'$  value rises suddenly. The highest ( $2498.001 \pm 122.21$  Pa) and the lowest ( $49.94 \pm 1.04$  Pa)

elastic modulus ( $G'$ ) at the end of the cooling period were obtained for SS and RS, respectively. The PS exhibited an intermediate value ( $1161.383 \pm 46.93$  Pa) for  $G'$ . The high amylose/amylopectin ratio corresponded to higher  $G'$  values, which is one of the significant factors of firmness in starch gels.

Increasing temperature leads to starch swelling and leaching out of amylose due to weakening H-bonds. Insignificant changes in  $G'$  implicate no gel-network formation. Also, disruption of starch granules due to limited swelling power and leaching out of amylose, leads to a sharp increase of  $G'$ .

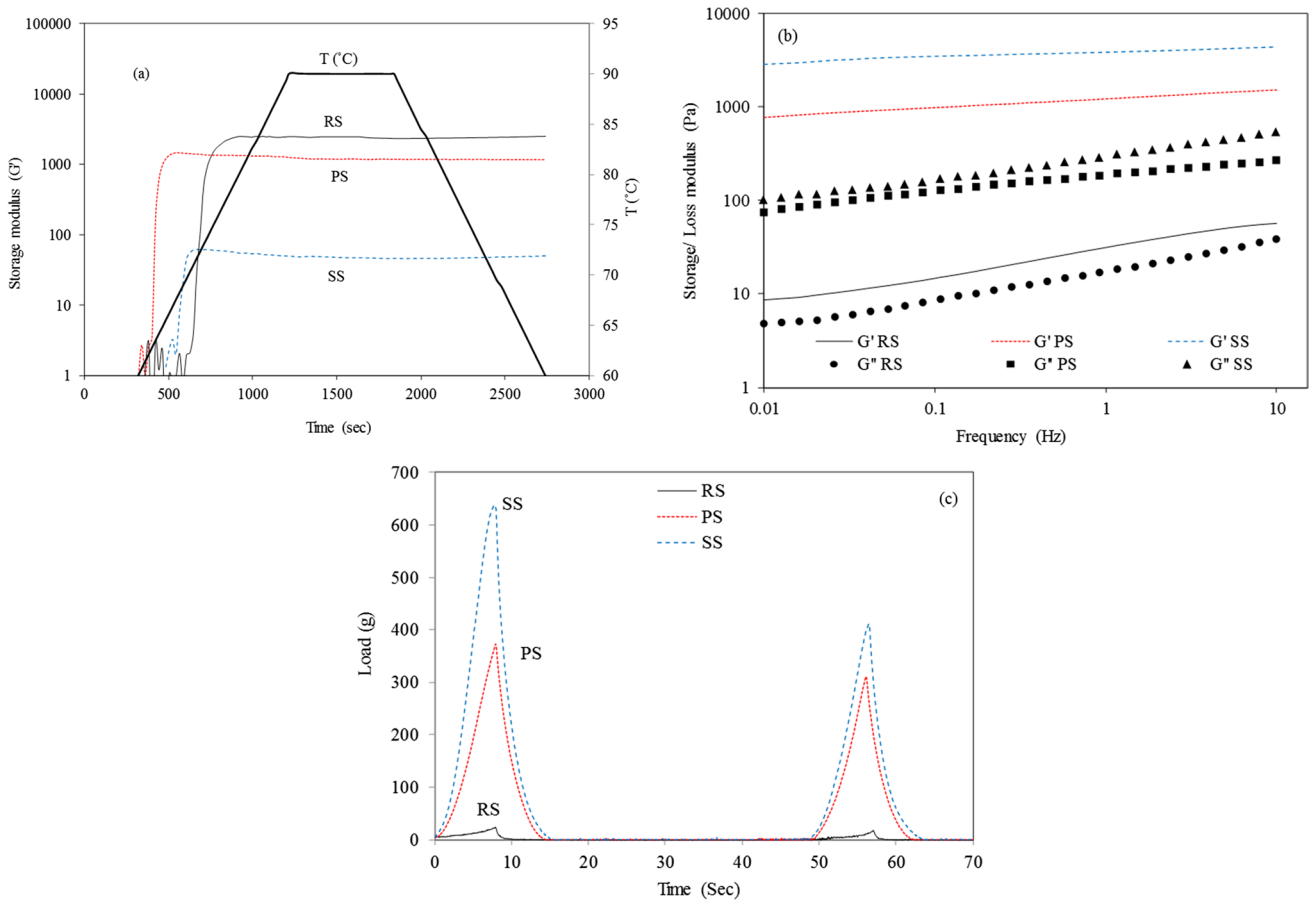


**Fig. 5** Storage modulus ( $G'$ ) during gel formation (15% w/v) as a function of temperature (a), dynamic rheological properties of starch gels (15% w/v) as a function of frequency (b), and texture profile analysis of starch gels (40%, w/v) (c)

Amylose forms junction zones that support the structure of the weak primary gel. In the equilibrium phase,  $G'$  quickly attains a steady value [14].

The mechanical spectrum for three starch gels at 60°C is presented in Fig. 5b. The predomination of elastic modulus ( $G'$ ) over viscous modulus ( $G''$ ) shows that all starch gels behaved as viscoelastic solids. The SS gel had the lowest 'n' value (0.056) while, 'n' values of 0.2968 and 0.096 were recorded for RS and PS gels, respectively. The elastic modulus was almost independent of frequency for SS and PS gels, evidenced by a slope (n) of logarithmic plots of  $G'$  versus frequency. Corn and potato starch gels also showed similar results at 25°C [38]. In all cases, the viscous modulus showed more frequency dependence which is associated with weak gel formation [39].

### Texture Profile Analysis of Starch Gels

TPA profiles for starch gel samples (40% w/v) are presented in Fig. 5c. The textural parameters varied significantly ( $p < 0.05$ ) and, SS exhibited the highest gel strength, gumminess, and resilience (Table 4). A minor adhesiveness was monitored in RS gel. The textural properties increased by increasing the concentration of starch gels from 10 to 40% (w/v), which indicate strong interactions among the constituents of starches at higher concentrations [14].

In starch gels, firmness is mainly caused by retrogradation, associated with the syneresis of water and the

crystallization of amylopectin. Starches with higher amylose content and longer amylopectin chains tend to make harder gels [40].

## Physicochemical Properties of Starch Film

### Light Transparency

However, low-transparent films may help increase the shelf life of some light-sensitive products. As presented in Table 5, SS films were the thickest (0.218 mm), while RS make the thinnest (0.136 mm) and the least heterogeneous films. The RS film was considerably more transparent, while the SS film was the least transparent and the most opalescent.

Lower amylose content causes a reduction in film thickness and heterogeneity. Also, the lower thickness may result from the lower viscosity of the film-forming suspension [41]. Other studies have shown that increases in the crystalline zone decreases the absorbance and increase the film transparency [42]; hence starch with low amylose content is expected to be more transparent.

### Film Stability in Water

Potential applications of starch-based films may require insolubility in water. However, for coatings or in encapsulation applications the water solubility is advantageous. As

**Table 4** Textural properties of studied starch gels

	Starch gel	Hardness (g)	Gumminess (g)	Cohesiveness	Springiness (mm)	Resilience	Adhesiveness (mJ)
SS	(10%, w/v)	102.00 ± 1.00 <sup>e</sup>	31.28 ± 1.45 <sup>e</sup>	0.30 ± 0.01 <sup>e</sup>	2.05 ± 0.03 <sup>b</sup>	0.34 ± 0.02 <sup>c</sup>	0.00 ± 0.00 <sup>b</sup>
	(20%, w/v)	265.66 ± 3.21 <sup>c</sup>	102.75 ± 5.16 <sup>c</sup>	0.38 ± 0.01 <sup>d</sup>	2.07 ± 0.01 <sup>b</sup>	0.39 ± 0.01 <sup>b</sup>	0.00 ± 0.00 <sup>b</sup>
	(40%, w/v)	632.00 ± 5.56 <sup>a</sup>	290.70 ± 5.88 <sup>a</sup>	0.46 ± 0.01 <sup>c</sup>	2.15 ± 0.02 <sup>a</sup>	0.53 ± 0.02 <sup>a</sup>	0.00 ± 0.00 <sup>b</sup>
PS	(10%, w/v)	63.33 ± 1.52 <sup>f</sup>	14.37 ± 1.63 <sup>f</sup>	0.22 ± 0.02 <sup>f</sup>	1.93 ± 0.03 <sup>c</sup>	0.27 ± 0.01 <sup>d</sup>	0.00 ± 0.00 <sup>b</sup>
	(20%, w/v)	135.00 ± 24.55 <sup>d</sup>	43.15 ± 7.61 <sup>d</sup>	0.32 ± 0.01 <sup>e</sup>	2.04 ± 0.02 <sup>b</sup>	0.32 ± 0.02 <sup>c</sup>	0.00 ± 0.00 <sup>b</sup>
	(40%, w/v)	334.33 ± 33.54 <sup>b</sup>	122.44 ± 10.52 <sup>b</sup>	0.36 ± 0.01 <sup>d</sup>	2.08 ± 0.00 <sup>b</sup>	0.40 ± 0.01 <sup>b</sup>	0.00 ± 0.00 <sup>b</sup>
RS	(10%, w/v)	10.66 ± 1.15 <sup>g</sup>	9.92 ± 1.17 <sup>f</sup>	0.91 ± 0.01 <sup>b</sup>	0.97 ± 0.03 <sup>e</sup>	0.07 ± 0.01 <sup>f</sup>	0.13 ± 0.05 <sup>a</sup>
	(20%, w/v)	14.66 ± 0.57 <sup>g</sup>	13.44 ± 0.39 <sup>f</sup>	0.93 ± 0.01 <sup>b</sup>	1.73 ± 0.07 <sup>d</sup>	0.13 ± 0.02 <sup>e</sup>	0.13 ± 0.05 <sup>a</sup>
	(40%, w/v)	25.00 ± 1.73 <sup>g</sup>	24.17 ± 0.71 <sup>e</sup>	0.97 ± 0.03 <sup>a</sup>	1.94 ± 0.02 <sup>c</sup>	0.25 ± 0.01 <sup>d</sup>	0.16 ± 0.50 <sup>a</sup>

Different letters within the same column represent significant differences ( $p < 0.05$ )

**Table 5** Mechanical properties of studied starch films

Parameters	SS	PS	RS
Thickness (mm)	0.216 ± 0.025 <sup>a</sup>	0.200 ± 0.010 <sup>a</sup>	0.133 ± 0.005 <sup>b</sup>
Transparency ( $A_{600}$ /mm)	0.909 ± 0.042 <sup>a</sup>	0.616 ± 0.015 <sup>b</sup>	0.523 ± 0.056 <sup>c</sup>
Stability in water (%)	37.76 ± 1.16 <sup>a</sup>	35.74 ± 1.44 <sup>b</sup>	31.62 ± 1.03 <sup>c</sup>
Elongation at break (E, %)	45.35 ± 1.89 <sup>c</sup>	73.20 ± 1.24 <sup>b</sup>	129.46 ± 6.21 <sup>a</sup>
Tensile strength (TS, MPa)	5.29 ± 0.24 <sup>a</sup>	3.86 ± 0.17 <sup>b</sup>	2.00 ± 0.06 <sup>c</sup>

Different letters within the same row represent significant differences ( $p < 0.05$ )

presented in Table 5, solubility in water is directly related to the amylose content. The water solubility values of the starch films were around 31–37% and, all films showed great integrity until the end of the solubility tests. The water solubility of 20% for tapioca starch films [43] and 38% for high amylose corn starch films [42] has been reported, regardless of the type and amount of plasticizer in film formulation.

### Mechanical Properties

The mechanical properties of starch films determine their suitability for specific applications and are affected by molecular weight, amylose content, film thickness, polymer chain packing, chain interaction, and film crystallinity [44]. As presented in Table 5, the maximum tensile strength varied from 2.00 to 5.29 MPa and elongation at break from 45.35 to 129.46%.

The results showed that SS with the highest amylose content has starch films with the highest maximum tensile strength but the lowest film stretchability (Table 5). Although these values are greatly dependent on the plasticizer content, thickness, water content, and additives, the same conclusion was reached by other researchers [45]. Another study also reported that films prepared from common maize starch had better maximum tensile strength than waxy starch due to their higher amylose content [46].

### Conclusion

The present study concluded the physicochemical and functional properties of saffron corm starch compared to potato and waxy rice starches. The lowest degree of crystallinity and also lowest gelatinization enthalpy are related to the higher amylose/amylopectin ratio of SS. The SS granules were irregular heterogeneous in shape and exhibited bimodal particle size distribution with a mean granule size of 8.87  $\mu\text{m}$ . The saffron corm starch showed the least swelling power and the most syneresis and paste turbidity. Also, the highest viscoelastic solid properties, gel strength, and final viscosity were obtained for SS. The elastic modulus of SS gel was less frequency dependent at 60°C. The thickest, the most heterogeneous and the least transparent films were prepared from the saffron corm starch. The films prepared by SS had the highest maximum tensile strength and stiffness but the lowest film stretchability. The results indicate that starch extracted from saffron corm can be used where stronger gelling properties are required or to prepare less transparent and stiffer films or coatings. Moreover, SS might be also used as a thickener and stabilizer in salad dressing preparations. Higher setback viscosity leads to higher

cohesiveness, hardness, lower stickiness and cooking loss, which gives probable suitability of SS application in noodles, too.

**Acknowledgements** The authors would like to acknowledge Research Institute of Food Science and Technology (RIFST) and Khorasan Razavi Agricultural and Natural Resources Research and Education Center.

**Author Contributions** All authors contributed to the study conception and design. The first draft of the manuscript was prepared by **Mozhgan Esmaeelian** and all authors commented on previous versions of the manuscript. All authors read and approved the final manuscript.

**Mozhgan Esmaeelian:** Investigation, Data curation, Writing—Original draft.

**Moslem Jahani:** Supervision, Methodology, Formal analysis, Investigation, Review and editing of the original draft.

**Javad Feizy:** Methodology, Resources, Review and editing of the original draft.

**Soodabeh Einafshar:** Review and edit the original draft.

**Funding** The authors do not receive a specific project grant but this work was supported by the block grant available to the Research Institute of Food Science and Technology (RIFST) received by Mozhgan Esmaeelian as a Ph. D candidate.

**Data Availability** All data generated or analysed during this study are included in this manuscript.

**Code Availability** A statement regarding code availability is not applicable.

### Declarations

**Competing Interests** The authors declare no competing interests.

**Ethical Approval** This article does not contain any studies with human or animal subjects.

**Consent to Participate** Not applicable.

**Consent for Publication** The authors hereby consent to the publication of the work.

**Conflict of Interest** The authors declare that they have no conflict of interest.

### References

1. B. Gong, W. Liu, H. Tan, D. Yu, Z. Song, L.A. Lucia, *Carbohydr. Polym.* **151**, 666–675 (2016). <https://doi.org/10.1016/j.carbpol.2016.06.010>
2. E.A. Esquivel-Fajardo, E.U. Martinez-Ascencio, M.E. Oseguera-Toledo, S.M. Londoño-Restrepo, M.E. Rodríguez-García, *Carbohydr. Polym.* **281**, 119048 (2022). <https://doi.org/10.1016/j.carbpol.2021.119048>
3. I. Chakraborty, P. N. S. S. Mal, U. C. Paul, M. H. Rahman, and N. Mazumder, *Food Bioprocess Technol* (2022). <https://doi.org/10.1007/s11947-022-02761-z>

4. J. Torruco-Uco, D. Betancur-Ancona, *Food Chem.* **101**, 1319–1326 (2007). <https://doi.org/10.1016/j.foodchem.2006.03.047>
5. C.G. Arp, M.J. Correa, C. Ferrero, *Food Bioprocess Technol.* **13**, 1181–1192 (2020). <https://doi.org/10.1007/s11947-020-02470-5>
6. J. Singh, O.J. McCarthy, H. Singh, *Carbohydr. Polym.* **64**, 569–581 (2006). <https://doi.org/10.1016/j.carbpol.2005.11.013>
7. I. Przetaczek-Roznowska, *Int. J. Biol. Macromol.* **101**, 536–542 (2017). <https://doi.org/10.1016/j.ijbiomac.2017.03.092>
8. A. M. Husaini, H. Badrul, M. Y. Ghani, J. A. Silva, and N. A. Kirmani, "Saffron (*Crocus sativus* Kashmirianus) cultivation in Kashmir: Practices and problems," in *Functional plant science and biotechnology*, A. M. Husaini, Ed., ed: Isleworth : Global Science Books, (2010)
9. M. Esmaeelian, M. Jahani, J. Feizy, S. Einafshar, *Food Anal. Method.* **14**, 74–87 (2021). <https://doi.org/10.1007/s12161-020-01855-8>
10. J. Bagri, A. Yadav, K. Anwar, J. Dkhar, S.L. Singla-Pareek, A. Pareek, *Sci Rep* **7**, 11904–11904 (2017). <https://doi.org/10.1038/s41598-017-10528-2>
11. J. Li, S. Zhang, Z. Zhang, S. Ren, D. Wang, X. Wang et al., *Int. J. Biol. Macromol.* **181**, 1023–1029 (2021). <https://doi.org/10.1016/j.ijbiomac.2021.04.127>
12. AOAC, "Official Methods of Analysis. 18th Edition," in *The Association of Official Analytical Chemists*, ed. Gaithersburg, MD, USA. (2005)
13. A.S. Babu, R. Parimalavalli, K. Jagannadham, J.S. Rao, *J. Food Sci. Technol.* **52**, 5745–5753 (2015). <https://doi.org/10.1007/s13197-014-1650-x>
14. M. Joshi, P. Aldred, S. McKnight, J.F. Panozzo, S. Kasapis, R. Adhikari et al., *Carbohydr. Polym.* **92**, 1484–1496 (2013). <https://doi.org/10.1016/j.carbpol.2012.10.035>
15. P. Vithu, S.K. Dash, K. Rayaguru, M.K. Panda, M. Nedunchezhiyan, *J. Food Meas. Charact.* **14**, 1520–1532 (2020). <https://doi.org/10.1007/s11694-020-00401-8>
16. F. Xu, L. Zhang, W. Liu, Q. Liu, F. Wang, H. Zhang et al., *Foods* **10**, 1–15 (2021). <https://doi.org/10.3390/foods10051104>
17. G. Hu, J. Chen, J. Gao, *Carbohydr. Polym.* **76**, 291–298 (2009). <https://doi.org/10.1016/j.carbpol.2008.10.032>
18. ASTM-D882–18, "Standard Test Method for Tensile Properties of Thin Plastic Sheeting," ed. Philadelphia, PA: American Society for Testing and Materials (2018)
19. L.A. Bello-Pérez, M.M. Sánchez-Rivera, C. Núñez-Santiago, S.L. Rodríguez-Ambríz, A.D. Román-Gutiérrez, *Carbohydr. Polym.* **81**, 63–69 (2010). <https://doi.org/10.1016/j.carbpol.2010.01.056>
20. R. T. Paraginski, N. L. Vanier, K. Moomand, M. de Oliveira, E. d. R. Zavareze, R. M. e Silva, et al., *Carbohydr. Polym.* **102**, 88–94 (2014). <https://doi.org/10.1016/j.carbpol.2013.11.019>
21. F.C.F. Galvez, A.V.A. Resurreccion, *J. Food Process. Preserv.* **17**, 93–107 (1993). <https://doi.org/10.1111/j.1745-4549.1993.tb00227.x>
22. A.M. Pascoal, M.C.B. Di-Medeiros, K.A. Batista, M.I.G. Leles, L.M. Lião, K.F. Fernandes, *Carbohydr. Polym.* **98**, 1304–1310 (2013). <https://doi.org/10.1016/j.carbpol.2013.08.009>
23. A.A. Wani, P. Singh, M.A. Shah, U. Schweiggert-Weisz, K. Gul, I.A. Wani, *Compr. Rev. Food Sci. Food Saf.* **11**, 417–436 (2012). <https://doi.org/10.1111/j.1541-4337.2012.00193.x>
24. M.E. Rodriguez-Garcia, M.A. Hernandez-Landaverde, J.M. Delgado, C.F. Ramirez-Gutierrez, M. Ramirez-Cardona, B.M. Millan-Malo et al., *Curr. Opin. Food Sci.* **37**, 107–111 (2021). <https://doi.org/10.1016/j.cofs.2020.10.002>
25. H.-Y. Kim, S. S. Park, and S.-T. Lim, *Colloids Surf. B* **126**, 607–620 (2015). <https://doi.org/10.1016/j.colsurfb.2014.11.011>
26. S.X. Tan, A. Andriyana, S. Lim, H.C. Ong, Y.L. Pang, G.C. Ngoh, *Polymers* **13**, 4398 (2021)
27. A. Xu, K. Guo, T. Liu, X. Bian, L. Zhang, C. Wei, *Molecules* **23**, 2135 (2018)
28. G.E. Vandeputte, R. Vermeylen, J. Geeroms, J.A. Delcour, *J. Cereal Sci.* **38**, 43–52 (2003). [https://doi.org/10.1016/S0733-5210\(02\)00140-6](https://doi.org/10.1016/S0733-5210(02)00140-6)
29. M.R. Debet, M.J. Gidley, *Carbohydr. Polym.* **64**, 452–465 (2006). <https://doi.org/10.1016/j.carbpol.2005.12.011>
30. B.Y. Ritika, B.S. Khatkar, B.S. Yadav, *Int. J. Food Prop.* **13**, 1339–1354 (2010). <https://doi.org/10.1080/10942910903131407>
31. N.G. Amani, A. Kamenan, A. Rolland-Sabaté, P. Colonna, *Afr. J. Biotechnol.* **4**, 94–101 (2005)
32. C. Perera, R. Hoover, *Food Chem.* **64**, 361–375 (1999). [https://doi.org/10.1016/S0308-8146\(98\)00130-7](https://doi.org/10.1016/S0308-8146(98)00130-7)
33. L. Novelo-Cen, D. Betancur-Ancona, *Starch - Stärke* **57**, 431–441 (2005). <https://doi.org/10.1002/star.200500398>
34. N. Singh Sodhi and N. Singh, *Food Chem.* **80**, 99–108 (2003). [https://doi.org/10.1016/S0308-8146\(02\)00246-7](https://doi.org/10.1016/S0308-8146(02)00246-7)
35. X. Luo, B. Cheng, W. Zhang, Z. Shu, P. Wang, X. Zeng, *CyTA—J Food* **19**, 532–540 (2021). <https://doi.org/10.1080/19476337.2021.1927194>
36. Z. Zhou, K. Robards, S. Helliwell, C. Blanchard, *Food Res. Int.* **40**, 209–214 (2007). <https://doi.org/10.1016/j.foodres.2006.10.006>
37. J. Loh, *J. Food Eng.* **16**, 75–90 (1992). [https://doi.org/10.1016/0260-8774\(92\)90021-W](https://doi.org/10.1016/0260-8774(92)90021-W)
38. Z. Yayuan, Z. Gu, H. Yan, Z. Li, L. Cheng, *Starch - Stärke* **63**, 11–16 (2011). <https://doi.org/10.1002/star.200900255>
39. I. Rosalina, M. Bhattacharya, *Carbohydr. Polym.* **48**, 191–202 (2002). [https://doi.org/10.1016/S0144-8617\(01\)00235-1](https://doi.org/10.1016/S0144-8617(01)00235-1)
40. F. Yamin, M. Lee, L. Pollak, P. White, *Cereal Chem.* **76**, 175–181 (1999). <https://doi.org/10.1094/CCHEM.1999.76.2.175>
41. E. Basiak, A. Lenart, F. Debeaufort, *Int. J. Biol. Macromol.* **98**, 348–356 (2017). <https://doi.org/10.1016/j.ijbiomac.2017.01.122>
42. M.A. Bertuzzi, M. Armada, J.C. Gottifredi, *J. Food Eng.* **82**, 17–25 (2007). <https://doi.org/10.1016/j.jfoodeng.2006.12.016>
43. S.R.B. Kim, Y.-G. Choi, J.-Y. Kim, S.-T. Lim, *LWT—Food Sci. Technol.* **64**, 475–482 (2015). <https://doi.org/10.1016/j.lwt.2015.05.009>
44. L. Dai, J. Zhang, F. Cheng, *Int. J. Biol. Macromol.* **132**, 897–905 (2019). <https://doi.org/10.1016/j.ijbiomac.2019.03.197>
45. A. Cano, A. Jiménez, M. Cháfer, C. González, A. Chiralt, *Carbohydr. Polym.* **111**, 543–555 (2014). <https://doi.org/10.1016/j.carbpol.2014.04.075>
46. V. de Almeida, B. Barretti, V. Ito, L. Malucelli, M.A. Carvalho, I. Demiate et al., *Mater. Res.* **23**, e20190576 (2020). <https://doi.org/10.1590/1980-5373-mr-2019-0576>

**Publisher's Note** Springer Nature remains neutral with regard to jurisdictional claims in published maps and institutional affiliations.